Identifying 850 *δ* Scuti pulsators in a narrow *Gaia* colour range with *TESS* 10-min full-frame images

Amelie K. Read,[1] Timothy R. Bedding [1][*] Prasad Mani [1] Benjamin T. Montet [2,3]
Courtney Crawford [1] Daniel R. Hey [4] Yaguang Li (李 亚光) [1,4] Simon J. Murphy [5] May
Gade Pedersen[1] and Joachim Kruger[5]

[1] *Sydney Institute for Astronomy, School of Physics, University of Sydney, Sydney, NSW 2006, Australia*
[2] *School of Physics, University of New South Wales, Sydney, NSW 2052, Australia*
[3] *UNSW Data Science Hub, University of New South Wales, Sydney, NSW 2052, Australia*
[4] *Institute for Astronomy, University of Hawai'i, Honolulu, HI 96822, USA*
[5] *Centre for Astrophysics, University of Southern Queensland, Toowoomba, QLD 4350, Australia*

ABSTRACT

We use *TESS* 10-min full-frame images (Sectors 27–55) to study a sample of 1708 stars within 500 pc of the Sun that lie in a narrow colour range in the centre of the δ Scuti instability strip ($0.29 < G_{\mathrm{BP}} - G_{\mathrm{RP}} < 0.31$). Based on the Fourier amplitude spectra, we identify 848 δ Scuti stars, as well as 47 eclipsing or contact binaries. The strongest pulsation modes of some δ Scuti stars fall on the period–luminosity relation of the fundamental radial mode but many correspond to overtones that are approximately a factor of two higher in frequency. Many of the low-luminosity δ Scuti stars show a series of high-frequency modes with very regular spacings. The fraction of stars in our sample that show δ Scuti pulsations is about 70 per cent for the brightest stars ($G < 8$), consistent with results from *Kepler*. However, the fraction drops to about 45 per cent for fainter stars and we find that a single sector of *TESS* data only detects the lowest amplitude δ Scuti pulsations (around 50 ppm) in stars down to about $G = 9$. Finally, we have found four new high-frequency δ Scuti stars with very regular mode patterns, and have detected pulsations in λ Mus that make it the fourth-brightest δ Scuti in the sky ($G = 3.63$). Overall, these results confirm the power of *TESS* and *Gaia* for studying pulsating stars.

Key words: parallaxes – stars: oscillations – stars: variables: Scuti.

1 INTRODUCTION

The *Transiting Exoplanet Survey Satellite* (*TESS*) is providing all-sky time-series space photometry at high cadence. In addition to pre-selected targets that may be observed at 120-s or 20-s cadence, the spacecraft takes full-frame images (FFIs). The cadence of the FFIs has been decreasing throughout the mission: they began at 30-min cadence, reduced to 10-min cadence, and are now being taken every 200 s. With these FFIs one can create custom light curves for any star falling on a *TESS* camera during any *TESS* observing sector.

One class of pulsating stars that has benefited enormously from the plentiful *TESS* data are the δ Scutis. These A/F type stars are abundant and are bright enough for high-quality *TESS* photometry. They pulsate with periods between $\sim$20 min and 5 h, hence even the highest frequency pulsators are well sampled by the 10-min FFIs. Further, with coherent oscillations that are only weakly damped, a single sector is sufficient to fully characterize them. Additional sectors are helpful to study any secular behaviour and to improve the overall signal-to-noise to detect any weak modes. Results on δ Scuti stars using *TESS* have included studies of individual stars

too numerous to list, as well as several studies of larger ensembles of pulsators (e.g. Antoci et al. 2019; Balona, Holdsworth & Cunha 2019; Balona & Ozuyar 2020; Barac et al. 2022; Skarka et al. 2022; Bedding et al. 2023; Daszyńska-Daszkiewicz et al. 2023; Li et al. 2023; Palakkatharappil & Creevey 2023; Pamos Ortega et al. 2023; Xue et al. 2023).

This paper looks at *TESS* photometry of stars in a narrow vertical strip in the colour–magnitude diagram that lies in the centre of the δ Scuti instability strip. This is a pilot study, which we plan to extend to a full all-sky survey. We make use of the 10-min FFIs that were taken in years 3 and 4 of the mission, which have a higher Nyquist frequency than the 30-min FFIs and have not yet been exploited for δ Scuti analyses.

2 METHODS AND RESULTS

2.1 Sample selection

We selected stars from the Gaia DR3 catalogue (Gaia Collaboration 2021) in a narrow colour range: $0.29 < G_{\mathrm{BP}} - G_{\mathrm{RP}} < 0.31$. This colour selection lies approximately in the centre of the observed δ Scuti instability strip (Bedding et al. 2023) and thus we expect a

[*] E-mail: tim.bedding@sydney.edu.au

significant proportion of stars to be pulsators. We limited our sample to stars within 500 pc of the Sun (parallax >2 mas) and apparent magnitude $G < 12$ (to exclude white dwarfs). Absolute magnitudes were calculated from Gaia DR3 apparent magnitudes and parallaxes, and no corrections were made for extinction or reddening.

To exclude *Gaia* solutions with spurious parallaxes, we removed 65 stars whose astrometric reliability diagnostic, `fidelity_v2`, calculated by Rybizki et al. (2022) was less than 0.75 (which was the threshold adopted by El-Badry et al. 2022). We also excluded two stars with spurious *Gaia* photometry (HD 79613B and HD 161740B), based on their values of `phot_bp_rp_excess_factor` (Riello et al. 2021) being much greater than 1 (the values are 70.2 and 8.5, respectively).

Our final *Gaia* sample contained 2844 stars. Of these, *TESS* 10-min FFI data were available for 1708 stars (60 per cent), from the third and fourth years of the mission (Cycles 3 and 4; Sectors 27–55). These 1708 stars define the sample that we have studied in this paper. For reference, we note that only half these stars (880 out of 1708) had 2-min *TESS* light curves, and so our use of FFIs has allowed us to obtain a much fuller sample that is essentially complete within its specified parameter space.

The upper panel of Fig. 1 shows the distribution of apparent *G* magnitudes of the *Gaia* sample (2844 stars) and the final *TESS* sample (1708 stars). The lower panel shows the Galactic *z* coordinate, calculated using the `astropy` function `coordinates.SkyCoord`. The exponential decline in number density with |z| is due to the vertical extent of the Milky Way disc (e.g. Rix & Bovy 2013). Fig. 2 shows the distribution in Galactic sky coordinates. The gap in *TESS* coverage reflects the fact that the spacecraft did not observe much of the ecliptic plane during Cycles 3 and 4.

2.2 Analysis of *TESS* light curves

Light curves corrected for systematic errors were extracted from the *TESS* FFIs using `eleanor` version 2.0.5 (Feinstein et al. 2019). For each star, we selected all sectors for which *TESS* obtained observations at 10-min cadence. We produced light curves using the default `eleanor` settings and the largest possible aperture (a 5×5 pixel box centred on the target), which we found to maximize the signal-to-noise ratio (SNR) of δ Scuti oscillations. We then selected the `eleanor` 'corrected flux' light curves, which removed long-period systematics that correlated with telescope pointing, time, or background levels. This served as a high-pass filter that removed variation slower than ∼1 d. Among our targets, 38 per cent were observed at 10-min cadence in more than one sector, and we stitched their light curves together and treated the combined observations as a single data set. Finally, we calculated the Fourier amplitude spectrum of each light curve up to a maximum frequency of $72\,\mathrm{d}^{-1}$, which is the Nyquist frequency of the 10-min *TESS* data.

2.3 Identification of δ Scuti stars

To identify δ Scuti pulsators, we followed a similar method to Murphy et al. (2019). For each Fourier spectrum, we calculated the skewness of the distribution of amplitudes for frequencies above $5\,\mathrm{d}^{-1}$. We have found this to be an excellent first step for identifying δ Scuti stars, since their Fourier spectra have a series of strong peaks amid a relatively flat distribution of background noise. We also measured the amplitude and SNR of the highest peak above $5\,\mathrm{d}^{-1}$, where the noise was measured as the mean amplitude at high frequencies (60–$70\,\mathrm{d}^{-1}$).
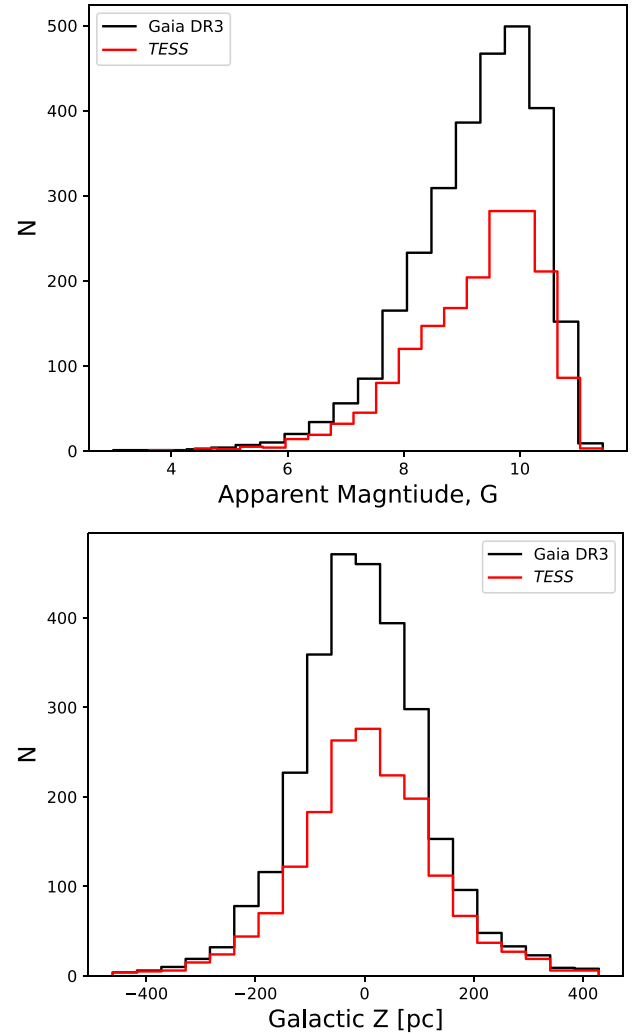

Figure 1. The black histograms show the distributions of the 2844 stars in our Gaia DR3 sample as a function of apparent magnitude (top) and distance from the Galactic plane (bottom). The lower (red) histograms show the 1708 stars that have 10-min *TESS* FFI light curves.
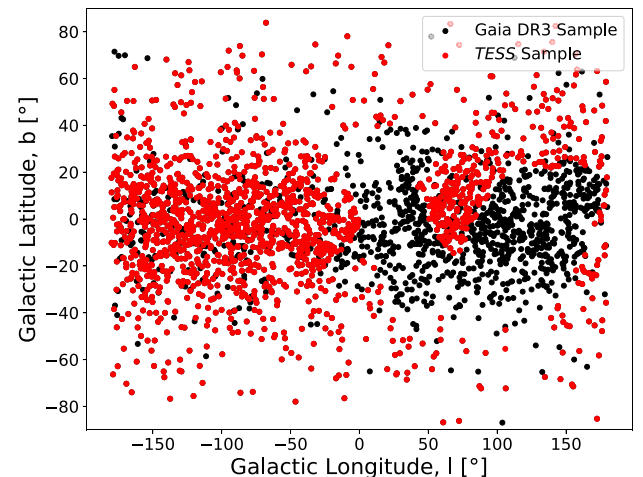

Figure 2. Distribution on the sky in Galactic coordinates of the 2844 Gaia DR3 stars in our sample (black points) and the 1708 stars with *TESS* 10-min light curves (red points).
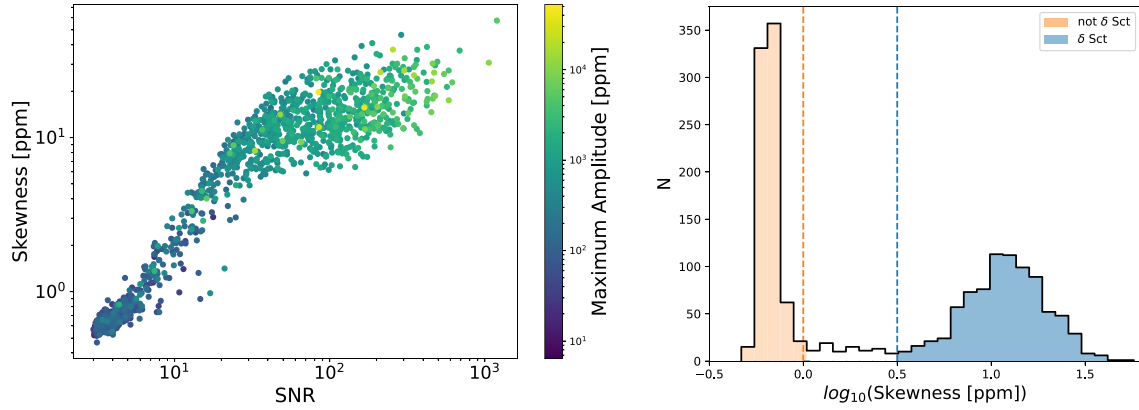
Figure 3. Left: Skewness of the amplitude spectrum above $5\,\mathrm{d}^{-1}$ for 1708 stars with 10-min *TESS* FFIs, versus the SNR of the highest peak above $5\,\mathrm{d}^{-1}$. The colour scale depicts the amplitude of this highest peak. Right: Histogram of the skewness measurements (see Section 2.2 for details).
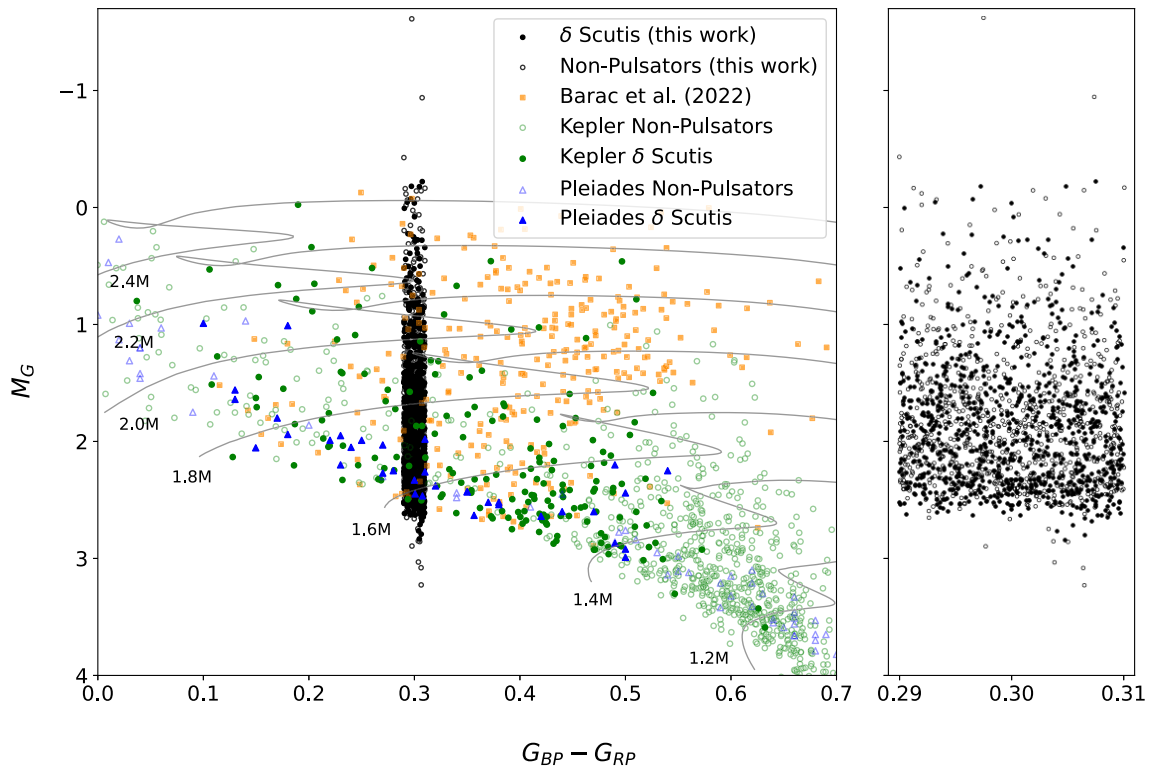

Figure 4. Left: *Gaia* colour–magnitude showing the sample of 1708 stars (black circles) lying in a narrow colour strip ($0.29 < G_{\mathrm{BP}} - G_{\mathrm{RP}} < 0.31$). Filled symbols show δ Scuti stars and open symbols are non-δ Scutis. The grey lines are evolutionary tracks with solar composition (Dotter 2016). The blue triangles are stars in the Pleiades open cluster studied by Bedding et al. (2023), the orange squares are 304 δ Scuti stars studied by Barac et al. (2022) that fall within 500 pc and the green circles are the *Kepler* sample studied by Murphy et al. (2019, see Section 3.3). Right: close-up showing the 1708 stars in our sample.

Fig. 3(a) shows the results, where skewness is plotted against the SNR of the highest peak (with peak amplitudes indicated by colour). The non-δ Scutis are grouped at the lower left, with low skewness and with a highest peak that has low SNR and is presumably due to noise. Stars at the upper right, with a skewness above $10^{0.5}$, are mostly δ Scuti stars. The 'neck' of stars connecting these groups, which contains about 5 per cent of the sample (Fig. 3b), are less clear-cut and we inspected these amplitude spectra to confirm their status. In many cases, the peaks above $5\,\mathrm{d}^{-1}$ were harmonics of peaks at lower frequency that arise from other types of variability, such as gravity and Rossby modes (Aerts 2021), and eclipsing or contact

binaries (Southworth 2021). We also used the period–luminosity relation that is followed by the fundamental radial mode of δ Scuti stars (Ziaali et al. 2019; Barac et al. 2022) as a guide of where to expect the lowest frequency p modes. In the end, we classified 59 of the 92 'neck' stars as δ Scuti pulsators. As a final check, we manually inspected all amplitude spectra and found a further seven stars that had been incorrectly labelled as δ Scutis (these were eclipsing or contact binaries).

Overall, from our sample of 1708 stars we identified 848 δ Scuti pulsators, as shown in Fig. 4 in a colour–magnitude diagram. We note that three stars in our sample are members of the Pleiades
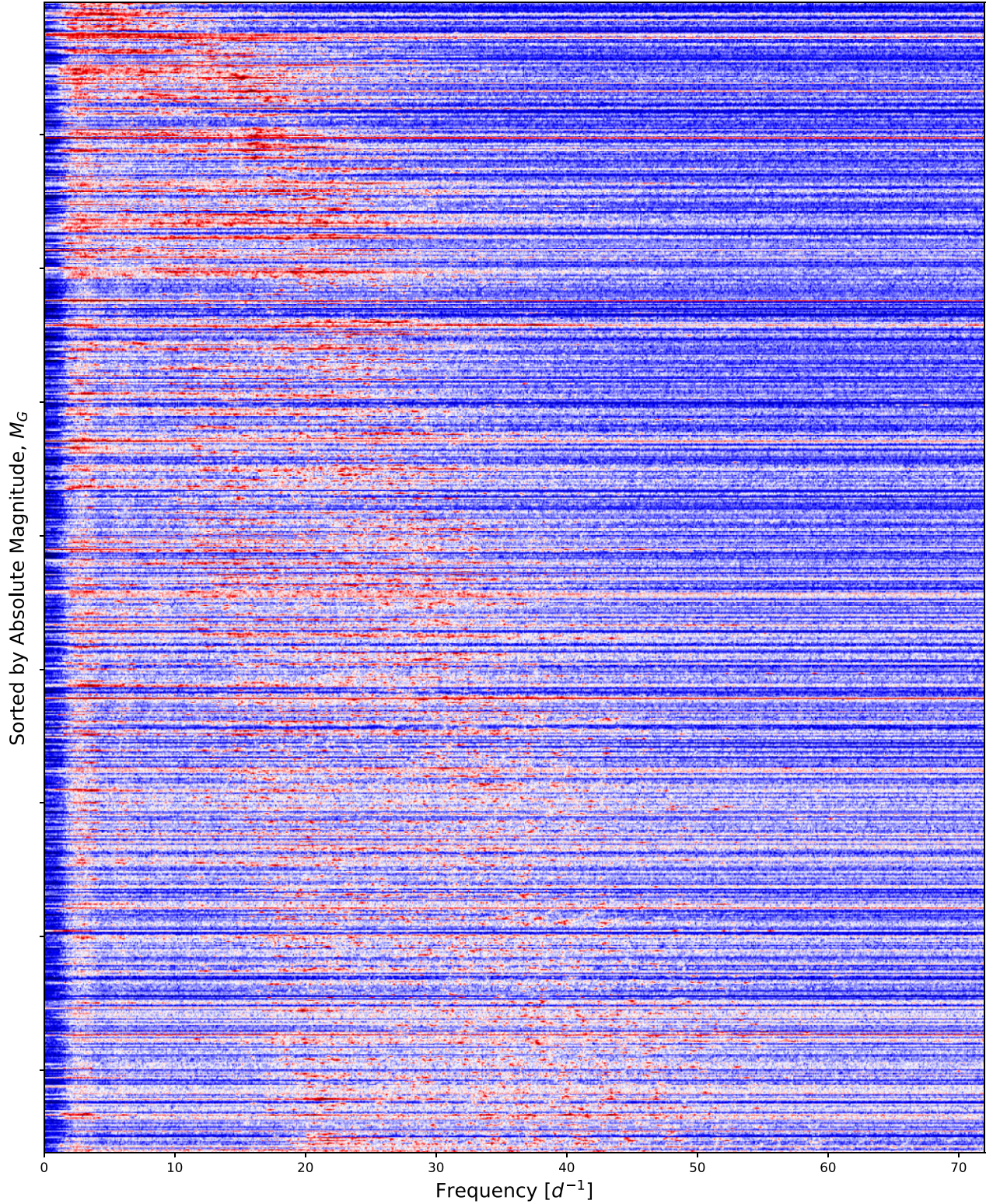
Figure 5. Stacked amplitude spectra for the 848 δ Scuti stars in our sample, sorted by absolute magnitude (brightest stars at the top of the diagram).

(HD 20655, V1228 Tau, and HD 23863; blue triangles in Fig. 4), as recently studied by Bedding et al. (2023). To check the reliability of our results, we cross-matched our sample with the 304 known δ Scuti stars studied using *TESS* 2-min light curves by Barac et al. (2022). Ten stars are in common and we successfully detected δ Scuti pulsations in all of them using the 200-s FFI light curves. We also identified 57 eclipsing or contact binaries in our sample, of which 11 show clear δ Scuti pulsations (Table 1) and 46 do not (Table 2). Two
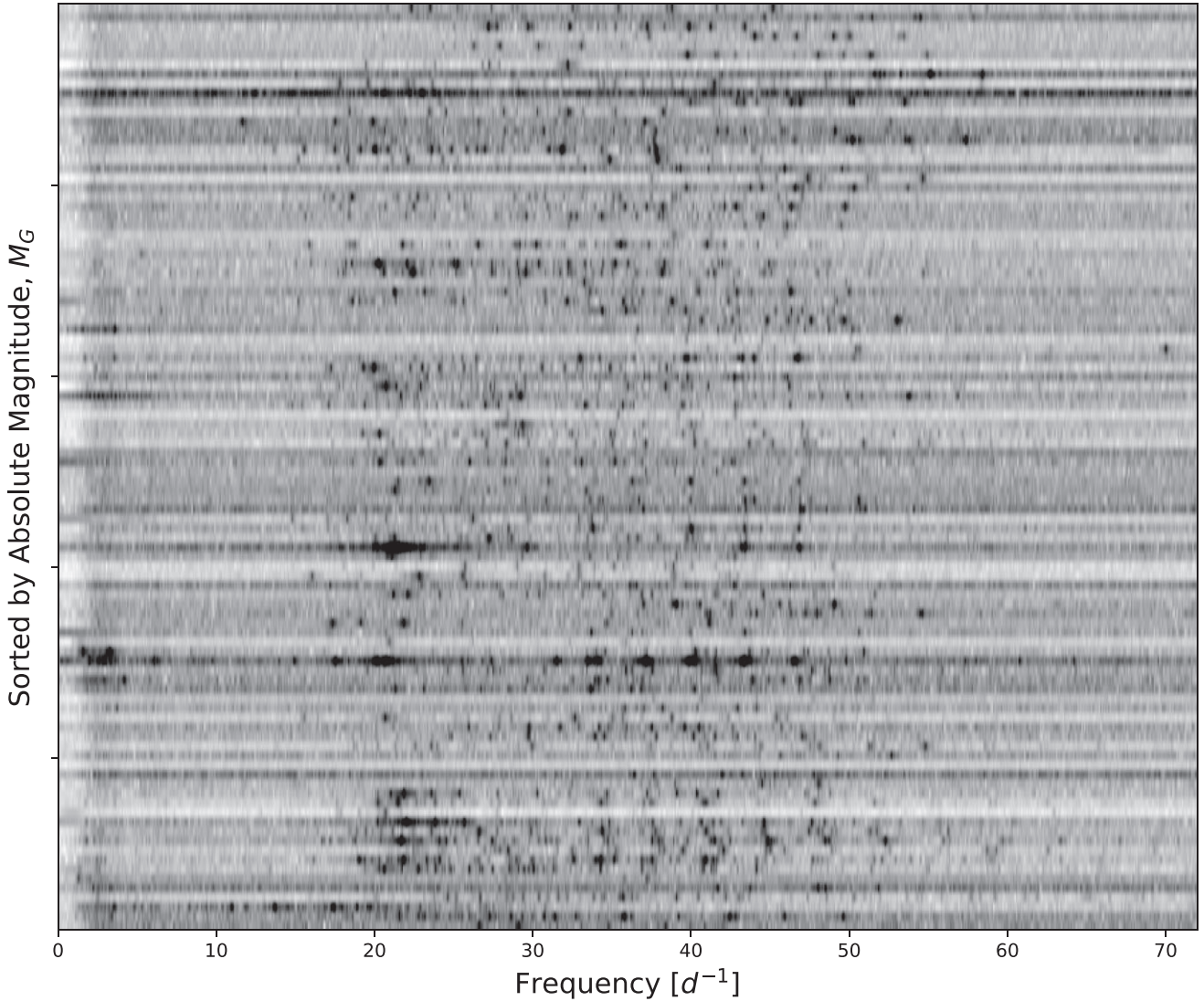
Figure 6. Stacked amplitude spectra from 0–72 d^{-1} (the Nyquist frequency) for the 100 least luminous δ Scuti stars. The spectra are sorted by absolute magnitude, with the brightest stars at the top of the diagram.

of the stars in Table 1 were previously known to be eclipsing binaries with a pulsating component: TIC 56127811 (HD 29972; Chen et al. 2022; Shi, Qian & Li 2022) and TIC 258351350 (HZ Dra; Chen et al. 2022).

3 DISCUSSION

3.1 Amplitude spectra

Our sample allows us to examine the properties of δ Scuti stars within a narrow temperature band as a function of luminosity. Fig. 5 shows the amplitude spectra of the 848 δ Scuti stars sorted according to absolute magnitude (M_{G}), with luminosity increasing from bottom to top. Note that the vertical stripes at 3, 6, 9, and 12 d^{-1} are artefacts caused by ringing from the high-pass filter in the `eleanor` pipeline (see Section 2.2). Apart from the feature at 3 d^{-1} (which is below the δ Scuti regime), these are very low-level and are barely visible in the individual amplitude spectra.

Overall, Fig. 5 confirms that the frequencies of δ Scuti stars decrease with increasing luminosity. This reflects the well-established property that the frequencies of p modes scale as the square root of stellar density (e.g. Aerts, Christensen-Dalsgaard & Kurtz 2010). Fig. 6 shows the subset of the 100 least luminous (and, therefore, predominantly the youngest) δ Scuti stars in the sample. We clearly see the regular patterns of high-frequency modes that were seen in similar plots using data from CoRoT (Michel et al. 2017) and *Kepler* (Bowman & Kurtz 2018), and were studied in detail for *TESS* stars by Bedding et al. (2020). Some examples are discussed in Section 3.4.

3.2 Period–luminosity relation

The trend in Fig. 5 of pulsation frequency decreasing with increasing luminosity can also be visualized in the period–luminosity (P–L) diagram. The δ Scuti P–L relation has previously been examined using parallaxes from Hipparcos (McNamara 1997, 2011), Gaia DR2 (Ziaali et al. 2019; Jayasinghe et al. 2020), and Gaia DR3 (Poro et al.
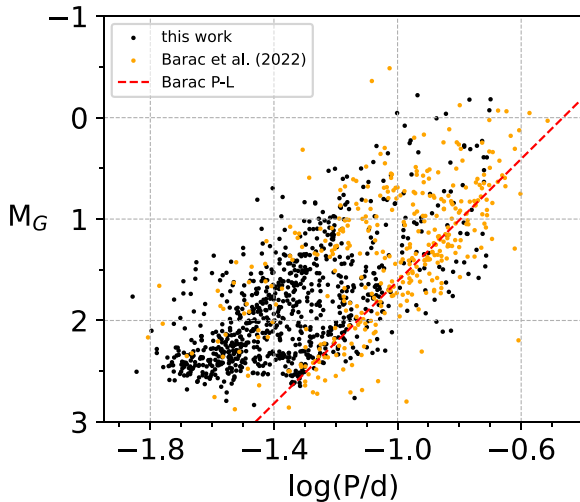
Figure 7. Period–luminosity relation for our sample of 848 δ Scuti stars (black circles) and 304 δ Scuti stars from the ground-based catalogues (Barac et al. 2022). The red line is the P–L relation fitted by Barac et al. (2022), which corresponds to the fundamental radial mode (see Section 3.2).
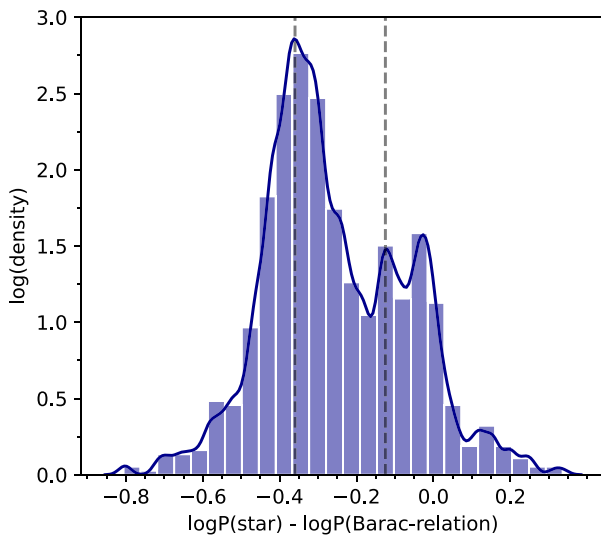

Figure 8. Histogram of the distance in $\log P$ of the 848 δ Scuti stars from the fundamental P–L relation, calculated as the horizontal distance from the red diagonal line in Fig. 7. Overlaid is a fixed-bandwidth KDE (solid line), which has peaks marked by vertical dashed lines (see Section 3.2).

2021; Barac et al. 2022; Gaia Collaboration 2023), and also in the Large Magellanic Cloud (Martínez-Vázquez et al. 2022).

The P–L relation for our sample is shown in Fig. 7 (black circles), which plots the absolute magnitude of each star versus the period of its dominant pulsation mode (the strongest peak above 5 d^{-1}). On the same figure, the orange symbols show 304 δ Scuti stars from ground-based catalogues (mainly Rodríguez, López-González & López de Coca 2000) that were studied by Barac et al. (2022), using parallaxes from Gaia DR3 and periods measured from *TESS* light curves.

The main P–L relation for δ Scuti stars corresponds to the fundamental radial mode (red line in Fig. 7, from Barac et al. 2022). This mode tends to be strong in higher amplitude stars (e.g. McNamara 2011), which explains why the relation is so clear in
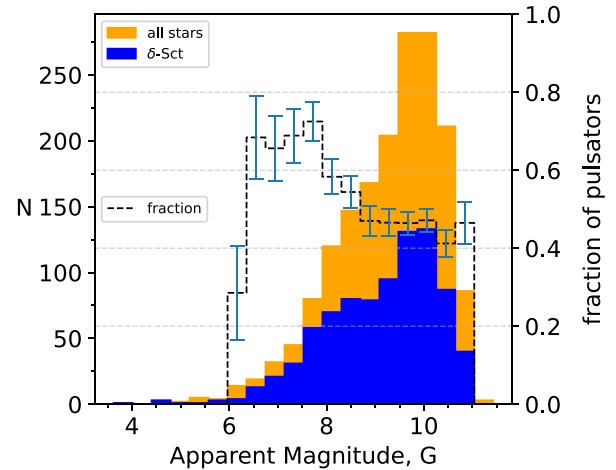

Figure 9. Histograms of apparent magnitude, *G*, for 848 δ Scuti stars (blue) out of a total sample of 1708 stars (orange). Referring to the right-hand axis, the fraction of δ Scuti pulsators in each bin is shown by the dashed black histogram.

catalogues compiled using ground-based light curves. Some of the stars in our sample do fall on this relation, but the majority lie to its left, indicating that they pulsate in higher overtones. Indeed, many of them fall on a second relation that is a factor of two shorter in period than the fundamental (-0.30 in $\log P$). This second ridge was first identified by Ziaali et al. (2019) and studied in more detail by Jayasinghe et al. (2020) and Barac et al. (2022). Interestingly, we find that the dominant peak in many of our stars lies on this second relation.

Fig. 8 shows a histogram of the horizontal distance of the 848 δ Scuti stars in our sample from the red diagonal line in Fig. 7, which is the P–L relation of the fundamental mode (Barac et al. 2022). Overlaid as a solid curve is a fixed-bandwidth KDE (kernel density estimate; Terrell & Scott 1992). We see a narrow excess of stars at a distance in $\log P$ of about -0.11 (a factor of 0.78), which we can identify with first-overtone pulsations (Petersen & Christensen-Dalsgaard 1996). The much larger peak at -0.35 corresponds to the second relation discussed above and indicates that the strongest mode in many low-amplitude δ Scuti stars is the third or fourth overtone, rather than the fundamental or the first overtone.

3.3 Fraction of pulsators

The fraction of stars within the δ Scuti instability strip that show pulsations was measured by Murphy et al. (2019) using the *Kepler* long-cadence (30-min) light curves. They found the fraction in the central region of the strip to be 50–70 per cent. Fig. 9 shows the 848 δ Scuti pulsators in our sample (blue histogram) and the total of 1708 stars (orange histogram) as a function of apparent *G* magnitude. The fraction of pulsators (dashed black histogram) is about 70 per cent for the brightest stars (*G* < 8), consistent with the *Kepler* result, but drops off for fainter stars. This implies that we are missing some pulsating stars at the fainter end of our *TESS* sample.

To investigate the completeness of our detections, Fig. 10 shows the amplitude of the highest peak in the Fourier spectrum of each star (above 5 d^{-1}), plotted as a function of apparent *G* magnitude. In the non-δ Scuti stars (open grey circles) this is a measure of the white noise, which is why we see a correlation with apparent magnitude. For the δ Scuti stars in our sample (filled black circles), most have
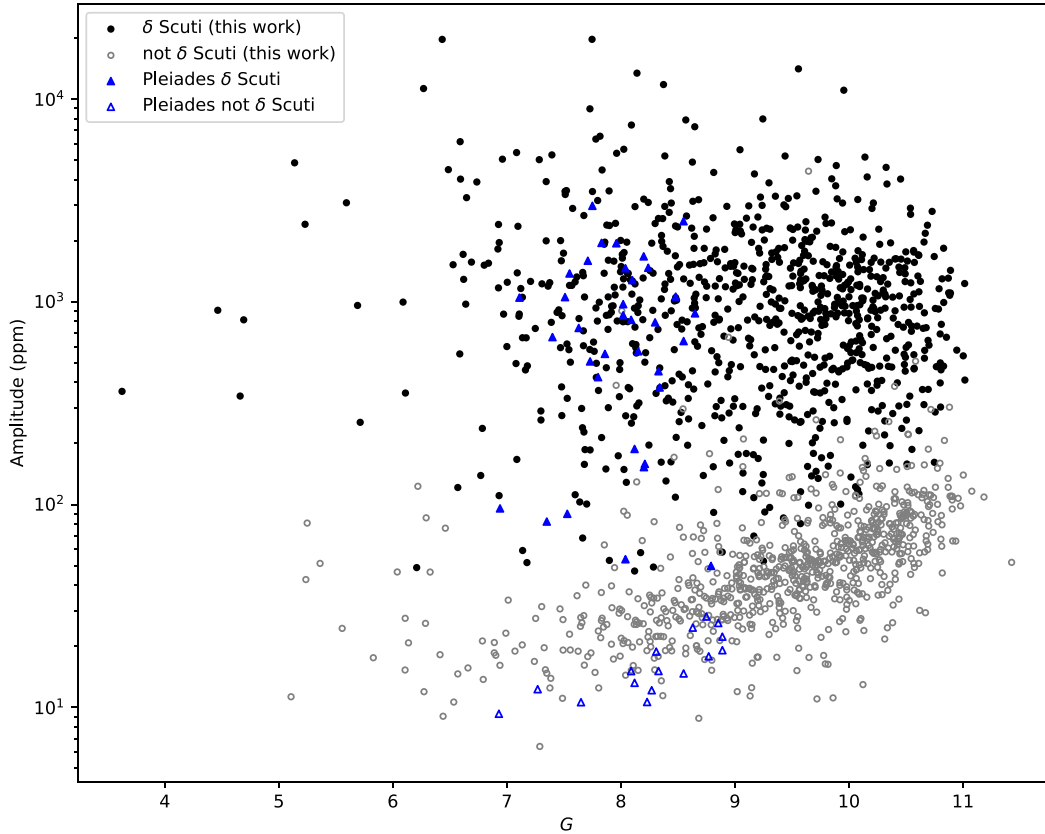
Figure 10. Amplitude of the highest peak in the Fourier spectrum above $5\,\mathrm{d}^{-1}$, plotted against apparent magnitude, G.
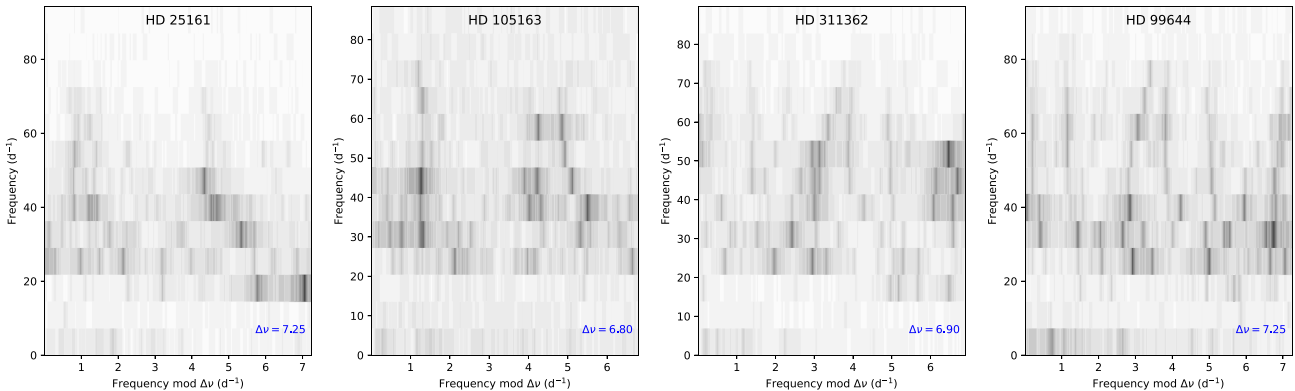

Figure 11. Amplitude spectra of four newly discovered high-frequency δ Scuti stars, shown in échelle format (see Bedding et al. 2020).

amplitudes in the range 300–3000 ppm.[1] The lowest amplitudes are around 50 ppm, but these are only detected in stars brighter than about $G = 9$. We can see from the distribution of points that we are probably missing some pulsators among the fainter stars ($G > 8$), as implied by the aforementioned drop in pulsator fraction in Fig. 9.

In Fig. 10 we also show the Pleiades sample studied by Bedding et al. (2023), restricted to the colour range in which pulsations occur ($0.1 < G_{\mathrm{BP}} - G_{\mathrm{RP}} < 0.55$). The non-$\delta$ Scuti stars (open blue triangles) have somewhat lower white-noise levels than our sample because the Pleiades was observed for three *TESS* sectors, whereas most of our sample have only one sector (keeping in mind we only included 10-min FFI data). The δ Scuti pulsators in the Pleiades (filled blue triangles) have amplitudes down to 50 ppm. In this case we can be fairly confident the Pleiades δ Scuti sample is complete at this amplitude level because (i) the Pleiades stars

---

[1]The open symbol in the upper right of Fig. 10 is from the star TIC 395181620 (HD 118476), whose light curve is contaminated by a nearby RR Lyrae (TIC 395181648; Clementini et al. 2019).
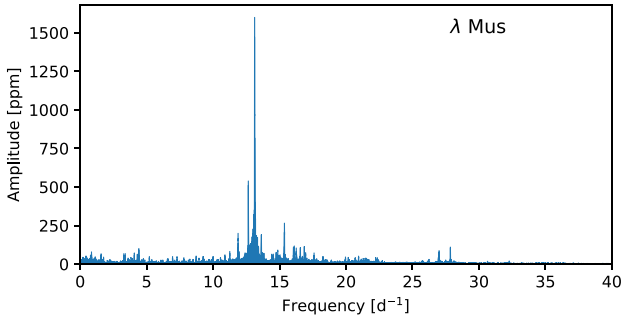
Figure 12. Amplitude spectrum of the bright δ Scuti star λ Mus, from the *TESS* 2-min light curve (Sectors 10, 11, 37, and 38). This star was not previously known to be a δ Scuti.
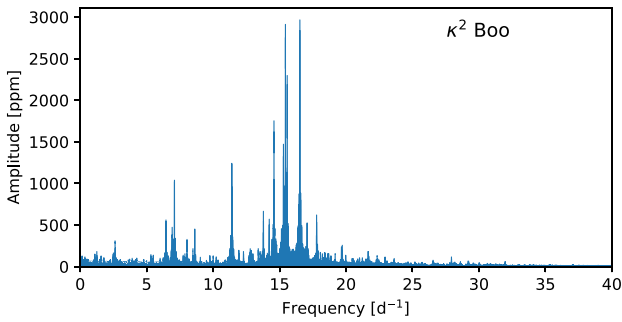

Figure 13. Amplitude spectrum of the bright δ Scuti star κ^2 Boo, from the *TESS* 2-min light curve (Sectors 22, 23, 49, and 50). The pulsations in this star were previously studied by Frandsen et al. (1995).

Table 1. List of 11 eclipsing or contact binaries that display δ Scuti pulsations.

TIC	Name	G
56127811	HD 29972	9.70
80106276	HD 67195	8.58
151238693		10.43
163559588	HD 100926	9.71
233976224	HD 262353	9.79
248990523		9.90
258351350	HZ Dra	8.09
279900855	HD 292098	9.36
306371075	HD 13018	6.59
394396270	HD 127472	10.21
463402815	HD 89160	10.17

are all brighter than $G = 9$, and (ii) the white noise level is lower (see above).

3.4 High-frequency δ Scuti stars

As mentioned in Section 3.1, our sample includes several δ Scuti stars with regular patterns of high-frequency modes (see Fig. 6). Nine of these are included in the sample of Bedding et al. (2020), namely HD 3622, HD 24975, HD 59594 (V349 Pup), HD 17341, HD 46722, HD 31640, HD 29783, HD 20203, and HD 55863. In addition, we have identified several new examples. Four with particularly regular oscillation patterns are shown in Fig. 11:

Table 2. List of 36 eclipsing or contact binaries that do not display obvious δ Scuti pulsations.

TIC	G	TIC	G
26858469	9.79	215336287	9.27
33520777	9.94	222020466	7.17
60658382	6.07	235187292	10.45
67043253	8.45	264899149	10.34
69459754	9.83	266735682	10.52
72852297	9.42	268404844	9.05
73945470	8.82	290146287	10.51
74528318	9.64	300955434	9.77
101417376	10.02	332337097	9.58
120689840	9.33	347081956	8.27
134907045	9.65	348830267	9.00
147972932	8.60	352342181	9.91
149846643	9.48	364398410	9.47
150443185	9.62	364965655	8.43
161840049	10.04	365065420	10.33
172903165	10.11	367436903	10.36
188573609	9.83	386588115	9.12
189475510	10.35	391461666	8.68
195612622	10.22	421285186	7.10
196052588	10.04	451878588	10.76
199549116	8.57	453620692	9.61
203652249	9.98	814744585	9.19
204318223	9.18	985576490	8.06

(i) TIC 14254276 (HD 25161), which is a member of the Taurus Association (Gagné et al. 2018).

(ii) TIC 86263305 (HD 105163), which does not appear to be a member of a moving group or association. We have obtained spectra of this star with Minerva Australis (Addison et al. 2019). From the 16 spectra taken on 9 nights, there is no evidence of a companion, either in radial velocities or in the line profiles. The spectra indicate a low $v\sin i$ of $11 \pm 7\,\mathrm{km\,s^{-1}}$, and an analysis of 84 Fe lines using iSpec (Blanco-Cuaresma et al. 2014; Blanco-Cuaresma 2019) shows $T_{\mathrm{eff}} = 7600 \pm 200\,\mathrm{K}$ and [Fe/H] $= -0.65 \pm 0.26$.

(iii) TIC 307035635 (HD 311362), which is in *TESS*'s southern continuous viewing zone and does not appear to be a member of a moving group or association

(iv) TIC 295882266 (HD 99644), which is a member of the Lower Centaurus-Crux (LCC) association (Gagné et al. 2018).

These are all good targets for further study and detailed modelling to determine stellar ages, by taking advantage of the fact that their regular patterns allow the modes to be identified (e.g. Pamos Ortega et al. 2022, 2023; Steindl, Zwintz & Müllner 2022; Murphy et al. 2023; Palakkatharappil & Creevey 2023; Scutt et al. 2023; Panda et al. 2024).

3.5 Notes on individual stars

3.5.1 λ Muscae: a new bright δ Scuti star

The star λ Mus has not previously been reported as variable but the *TESS* data clearly shows δ Scuti pulsations (Fig. 12). Its apparent magnitude of $V = 3.65$ ($G = 3.62$) makes λ Mus the fourth-brightest known δ Scuti, behind α Aql (Altair; $V = 0.76$; Buzasi et al. 2005), ρ Pup ($V = 2.81$; Eggen 1956), and γ Boo ($V = 3.02$; Guthnick & Fischer 1940). Based on its absolute magnitude, the fundamental radial mode of λ Mus should be at about $4.5\,\mathrm{d^{-1}}$, and so the strongest mode at $13.12\,\mathrm{d^{-1}}$ is presumably a higher overtone.

3.5.2 κ^2 *Bootis: a bright evolved δ Scuti star*

The star κ^2 Boo is the second brightest δ Scuti pulsator in our sample, and was studied in detail by Frandsen et al. (1995). The *TESS* data confirm the pulsations (Fig. 13). Based on its absolute magnitude, the fundamental radial mode of κ^2 Boo should be at about $5.8 \, \mathrm{d}^{-1}$, and so the strongest modes at $15–16 \, \mathrm{d}^{-1}$ must be overtones.

4 CONCLUSIONS

We used Gaia DR3 to select a sample of 2844 stars within 500 pc of the Sun that lie in a narrow colour range in the centre of the δ Scuti instability strip ($0.29 < G_{\mathrm{BP}} - G_{\mathrm{RP}} < 0.31$). For 1708 of these stars, *TESS* 10-min FFIs (Sectors 27–55) are available and we used the `eleanor` package (Feinstein et al. 2019) to extract light curves. Using Fourier amplitude spectra, we identified 848 δ Scuti stars, as well as 47 eclipsing or contact binaries (Tables 1 and 2).

The pulsation frequencies of the δ Scuti stars decrease with increasing luminosity (Fig. 5), which reflects the well-established property that the frequencies of pressure modes scale as the square root of stellar density. When we consider the strongest mode in each star, some fall on the P–L relation of the fundamental radial mode but many correspond to overtones that are approximately a factor of two higher in frequency (Figs 7 and 8). Many of the low-luminosity δ Scuti stars show a series of high-frequency modes (Fig. 6), including four new examples with very regular spacings (Fig. 11).

The fraction of stars in our sample that show δ Scuti pulsations (Fig. 9) is about 70 per cent for the brightest stars ($G < 8$), consistent with results from *Kepler* (Murphy et al. 2019). However, for fainter stars the fraction drops to about 45 per cent, indicating that we are missing some pulsating stars at the fainter end. This is confirmed by Fig. 10, which shows that a single sector of *TESS* data only detects the lowest amplitude δ Scuti pulsations (around 50 ppm) in stars down to about $G = 9$.

Overall, these results confirm the power of *TESS* and *Gaia* for studying pulsating stars. We plan to expand this work to encompass the entire *TESS* data set across the whole instability strip.

DATA AVAILABILITY

The *TESS* data underlying this article are available at the MAST Portal (Barbara A. Mikulski Archive for Space Telescopes), at https://mast.stsci.edu/portal/Mashup/Clients/Mast/Portal.html

REFERENCES

Addison B. et al., 2019, PASP, 131, 115003
Aerts C., 2021, Rev. Mod. Phys., 93, 015001
Aerts C., Christensen-Dalsgaard J., Kurtz D. W., 2010, Asteroseismology. Springer, Berlin
Antoci V. et al., 2019, MNRAS, 490, 4040
Astropy Collaboration, 2013, A&A, 558, A33
Astropy Collaboration, 2018, AJ, 156, 123
Balona L. A., Ozuyar D., 2020, MNRAS, 493, 5871
Balona L. A., Holdsworth D. L., Cunha M. S., 2019, MNRAS, 487, 2117
Barac N., Bedding T. R., Murphy S. J., Hey D. R., 2022, MNRAS, 516, 2080
Bedding T. R. et al., 2020, Nature, 581, 147
Bedding T. R. et al., 2023, ApJ, 946, L10
Blanco-Cuaresma S., 2019, MNRAS, 486, 2075
Blanco-Cuaresma S., Soubiran C., Heiter U., Jofré P., 2014, A&A, 569, A111
Bowman D. M., Kurtz D. W., 2018, MNRAS, 476, 3169
Buzasi D. L. et al., 2005, ApJ, 619, 1072
Chen X. et al., 2022, ApJS, 263, 34
Clementini G. et al., 2019, A&A, 622, A60
Daszyńska-Daszkiewicz J., Walczak P., Pamyatnykh A., Szewczuk W., Niewiadomski W., 2023, ApJ, 942, L38
Dotter A., 2016, ApJS, 222, 8
Eggen O. J., 1956, PASP, 68, 238
El-Badry K., Conroy C., Fuller J., Kiman R., van Roestel J., Rodriguez A. C., Burdge K. B., 2022, MNRAS, 517, 4916
Feinstein A. D. et al., 2019, PASP, 131, 094502
Frandsen S., Jones A., Kjeldsen H., Viskum M., Hjorth J., Andersen N. H., Thomsen B., 1995, A&A, 301, 123
Gagné J., Roy-Loubier O., Faherty J. K., Doyon R., Malo L., 2018, ApJ, 860, 43
Gaia Collaboration, 2021, A&A, 649, A1
Gaia Collaboration 2023, A&A, 674, A36
Guthnick P., Fischer H., 1940, Astron. Nachr., 271, 81
Harris C. R. et al., 2020, Nature, 585, 357
Hunter J. D., 2007, Comput. Sci. Eng., 9, 90
Jayasinghe T. et al., 2020, MNRAS, 493, 4186
Li G. et al., 2023, preprint (arXiv:2311.16991)
Lightkurve Collaboration 2018, Lightkurve: Kepler and TESS time series analysis in Python, Astrophysics Source Code Library, record ascl:1812.013
Martínez-Vázquez C. E., Salinas R., Vivas A. K., Catelan M., 2022, ApJ, 940, L25
McNamara D., 1997, PASP, 109, 1221
McNamara D. H., 2011, AJ, 142, 110
Michel E. et al., 2017, EPJ Web Conf., 160, 03001
Murphy S. J., Hey D., Van Reeth T., Bedding T. R., 2019, MNRAS, 485, 2380
Murphy S. J., Bedding T. R., Gautam A., Joyce M., 2023, MNRAS, 526, 3779
Palakkatharappil D. B., Creevey O. L., 2023, A&A, 674, A146
Pamos Ortega D., García Hernández A., Suárez J. C., Pascual Granado J., Barceló Forteza S., Rodón J. R., 2022, MNRAS, 513, 374
Pamos Ortega D., Mirouh G. M., García Hernández A., Suárez Yanes J. C., Barceló Forteza S., 2023, A&A, 675, A167
Panda S. K., Dhanpal S., Murphy S. J., Hanasoge S., Bedding T. R., 2024, ApJ, 960, 94
Petersen J. O., Christensen-Dalsgaard J., 1996, A&A, 312, 463
Poro A. et al., 2021, PASP, 133, 084201
Riello M. et al., 2021, A&A, 649, A3
Rix H.-W., Bovy J., 2013, A&AR, 21, 61
Rodríguez E., López-González M. J., López de Coca P., 2000, A&AS, 144, 469
Rybizki J. et al., 2022, MNRAS, 510, 2597
Scutt O. J., Murphy S. J., Nielsen M. B., Davies G. R., Bedding T. R., Lyttle A. J., 2023, MNRAS, 525, 5235
Shi X.-d., Qian S.-b., Li L.-J., 2022, ApJS, 259, 50
Skarka M. et al., 2022, A&A, 666, A142

Southworth J., 2021, Universe, 7, 369

Steindl T., Zwintz K., Müllner M., 2022, A&A, 664, A32

Terrell G. R., Scott D. W., 1992, Ann. Stat., 20, 1236

Virtanen P. et al., 2020, Nat. Methods, 17, 261

Xue W., Niu J.-S., Xue H.-F., Yin S., 2023, Res. Astron. Astrophys., 23, 075002

Ziaali E., Bedding T. R., Murphy S. J., Van Reeth T., Hey D. R., 2019, MNRAS, 486, 4348

This paper has been typeset from a TEX/LATEX file prepared by the author.